Steering in Scale Space to Optimally Detect Image Structures

Jeffrey Ng and Anil A. Bharath

Faculty of Engineering,
Imperial College London,
United Kingdom SW7 2AZ
{jeffrey.ng,a.bharath}@imperial.ac.uk

Abstract. Detecting low-level image features such as edges and ridges with spatial filters is improved if the scale of the features are known *a priori*. Scale-space representations and wavelet pyramids address the problem by using filters over multiple scales. However, the scales of the filters are still fixed beforehand and the number of scales is limited by computational power. The filtering operations are thus not adapted to detect image structures at their optimal or intrinsic scales. We adopt the steering approach to obtain filter responses at arbitrary scales from a small set of filters at scales chosen to accurately sample the "scale space" within a given range. In particular, we use the Moore-Penrose inverse to learn the steering coefficients, which we then regress by polynomial function fitting to the scale parameter in order to steer the filter responses continuously across scales. We show that the extrema of the polynomial steering functions can be easily computed to detect interesting features such as phase-independent energy maxima. Such points of energy maxima in our α-scale-space correspond to the intrinsic scale of the filtered image structures. We apply the technique to several well-known images to segment image structures which are mostly characterised by their intrinsic scale.

1 Introduction

Low-level feature detection and extraction by spatial filters is used in many fields such as image analysis, image representation, image compression and computer vision. In applications where the aim of the spatial filtering is to reconstruct the original image, e.g. compression, the choice of filter size and scale affect the spatial frequency of the encoded and reconstructed image structures. A set of filters at different scales can be employed to encode coarse, medium and fine structures in the image [1]. However, an image structure may contribute significantly to multiple filter responses over different scales when the filter scale does not match the scale of the image structure. While this does not affect the reconstruction process, inferring the presence of low-level features from filter responses becomes difficult because of the ambiguity arising from the sub-optimal encoding of image structures and the possible encoding of multiple structures into a single filter response when incorrect filter scales are used.

T. Pajdla and J. Matas (Eds.): ECCV 2004, LNCS 3021, pp. 482–494, 2004.

The problem of incorrect filter scale has previously been addressed by filtering over a greater number of finely-sampled scales. Fdez-Valdivia [2] constructed a bank of 2D Gabor filters over multiple orientations and scales and used the normalised 2D power spectrum over the filter responses to detect activation at scales where image structures exist. Lindeberg [3] uses extrema over scales in normalised scale-space to optimally detect image structures at their intrinsic scale. Kadir and Brady [4] have shown that normalised maxima of entropy of low-level features in images can be used to detect salient image structures. There is also evidence that neurons in the primary visual cortex of Old World monkeys "tune" their spatial frequency response over time to detect features from coarse to fine scale [5]. This spatial frequency tuning highlights the importance of searching over a range of scales to optimally detect image features.

The main problem with these approaches is that exhaustive filtering with kernels over a wide range of finely-sampled scales is computationally intensive and inefficient. Fast implementations of scale selection by searching for scale-space maxima has been proposed by [6,7] using quadratic interpolation of the filter responses across scales. On the other hand, Freeman and Adelson [8] devised an analytical method for linearly combining all the responses of a small set of oriented basis filters to obtain filter responses over all orientations. While linearly combining the basis filter responses over orientations results in a Taylor series expansion, an analytical formulation for steering filter responses across the scale parameter is not so forthcoming because of the unbounded nature of the problem, i.e. filter scales can theoretically increase to infinity. In practice, the maximum filter scale is limited by the size of the image. Perona [9] used the Singular Value Decomposition to design scale-steerable "deformable" filters. Bharath [10] constructed exemplar vectors of the radial frequency response of filters across scales and used a Moore-Penrose generalised inverse to learn the steering coefficients through simple matrix algebra. We modify the technique by learning the steering coefficients from radial response exemplars in the spatial domain and we parameterise the coefficients in terms of scale through regressive fitting of polynomial functions.

In Section 2, we describe a method for specifying the angular and radial frequency characteristics of filter kernels in the Fourier domain to construct an appropriate scale-space and then generating filter mask coefficients in the spatial domain by the inverse discrete Fourier transform. In Section 3, we exploit the ability to synthesise filters of arbitrary radial frequency responses and thus spatial scale in order to build two exemplar matrices containing desired radial responses in the spatial domain over a finely-sampled range of scales and over a small fixed set of basis scales respectively. We use the Moore-Penrose inverse to learn the linear combination coefficients to compute the former from the latter. The linear combination coefficients are then parameterised over scale by polynomial functions, yielding continuous scale steering functions. After filtering an image, we collapse in Section 4 the fields of filter responses of the basis set and the individual polynomial steering functions for each basis filter into a two-dimensional field of single polynomial steering functions. The maxima of these single polynomial steering functions can be easily obtained by computing

the roots of their derivative. Although we cannot directly steer the energy of a pair of complex filters in quadrature using this method, we can still compute the location of the maxima of the square of the energy which is the same as the location of the maxima of the energy. We show that such energy maxima correspond to the intrinsic scale of the image structure being filtered in a similar manner to [2,3,4]. We finally show how the scale at which energy maxima occurs in an image can be used to segment a class of well-known natural images where intrinsic scale plays an important role in defining structures in the image.

2 Design of Polar Separable Filters

Characteristics of local low-level image structures at any position consist of orientation, scale and phase [9]. In order to detect such structures, spatial filters are designed with similar orientation, scale and phase characteristics. To steer through the scale parameter, we need to design filters where the other parameters are kept constant. Polar separable filter kernels allow the radial frequency (scale) characteristic of the filters to be separately specified from the angular frequency (orientation) characteristic [11]. Furthermore, filtering with pairs of filter kernels in quadrature, where one filter is the Hilbert transform of the other, yields a phase-independent "energy" response.

The polar separable filter kernel $G_\alpha^\theta(\omega, \phi)$ is specified in the Fourier domain by the radial frequency function $G_\alpha(\omega)$ and angular frequency function $G^\theta(\phi)$ where α and θ are the scale and orientation of the desired filter respectively

$$G_\alpha^\theta(\omega, \phi) = G_\alpha(\omega)G^\theta(\phi) \tag{1}$$

The angular frequency characteristic of the filter affects the selectivity of its response to a specific range of orientations of image structures. The angular power (sum of squares) of a set of oriented filters for covering orientations $[0, \pi]$ also needs to be flat in order to provide uniform coverage. We choose a third power cosine function, clipped by a rectangular function, which gives a flat angular power response when used in a set of four orientations, i.e. $\theta \in \{0, \frac{\pi}{4}, \frac{\pi}{2}, \frac{3\pi}{4}\}$

$$G^\theta(\phi) = cos^3(\phi - \theta)rect(\phi - \theta) \tag{2}$$

where *rect* is the unit rectangular function

$$rect(\phi) = \begin{cases} 1 \text{ , if } |\phi| \leq \frac{\pi}{2} \\ 0 \text{ , otherwise} \end{cases} \tag{3}$$

The radial frequency characteristic of the filter affects the spread of its power spectra over scales. Traditional linear scale-space representations use derivatives of Gaussian in the spatial domain [12]. However, the amplitude of Gaussian spatial derivatives decrease over scales for scaled versions of the same image structure, rendering comparison of filter responses across scales more complex. Lindeberg [3] thus introduces an L_p normalisation of the scale-space filter responses so that their maxima corresponds to the optimal detection of image

structures at their intrinsic scale. On the other hand, Poisson kernels have recently been investigated for the consistency of filter behaviour over scales [13]. We adopt Erlang functions [14] of order $n = 7$ and scale α, which possess similar radial frequency responses to Poisson kernels and also benefit from quasi-invariant energy response over scales α avoiding the need for scale normalisation (which we do not show here due to lack of space)

$$G_\alpha(\omega) = \left(\frac{\alpha e}{n}\right)^n \omega^n e^{-\alpha\omega} \tag{4}$$

The inverse discrete Fourier transform of $G^\theta_\alpha(\omega, \phi)$ yields a complex filter $g^\theta_\alpha(\omega, \phi)$ in the spatial domain where the real and imaginary parts of the kernel are in quadrature. The magnitude of the response of this complex filter, when convolved with an image, provides a phase-independent "energy" response [11]. Following this approach, complex filter kernels of arbitrary orientation and scale can be synthesised.

3 Steering in Scale

A family of spatial filter kernels with similar orientation but varying scales can be obtained by varying the α scale parameter in Eqn (4). A scale-space representation similar to [1] can easily be constructed, providing a continuum of filter responses across scales. However, filtering at very small scale intervals to obtain a continuum of filter responses is a computationally intensive operation. Perona [9] approached the problem of designing a steerable basis filter set by first choosing the number of filters and thus the number of filtering operations. Then, Singular Value Decomposition is used to synthesise the best filter kernels for a certain detection task such as steering across scales. In contrast, we start with polar separable filter kernels where the desired orientation and radial characteristics are pre-specified and use the method of Bharath [15] to find the steering coefficients. Bharath generated radial frequency responses across many scales at very fine intervals and used a Moore-Penrose generalised inverse to learn the steering coefficients for obtaining those responses from the linear combination of a small set of basis filters. He varied both the scale parameter α and the order n of the Erlang functions in order to construct his basis set.

To create steerable filters, we first assume that the steering of filter responses across scales can be obtained by linearly combining the responses $f^\theta_{\alpha_i}(x, y)$, where $i \in \{1, \ldots, N\}$, of a small set of N basis filters $G^\theta_{\alpha_i}(x, y)$ as

$$f^\theta_\alpha(x, y) = \sum_{i=1}^{N} s_{i,\alpha} f^\theta_{\alpha_i}(x, y) \tag{5}$$

where $s_{i,\alpha}$ is the steering coefficient of filter i for scale α. We can also formulate Eqn (5) into matrix form

$$\mathbf{F} = \mathbf{F_B S} \tag{6}$$

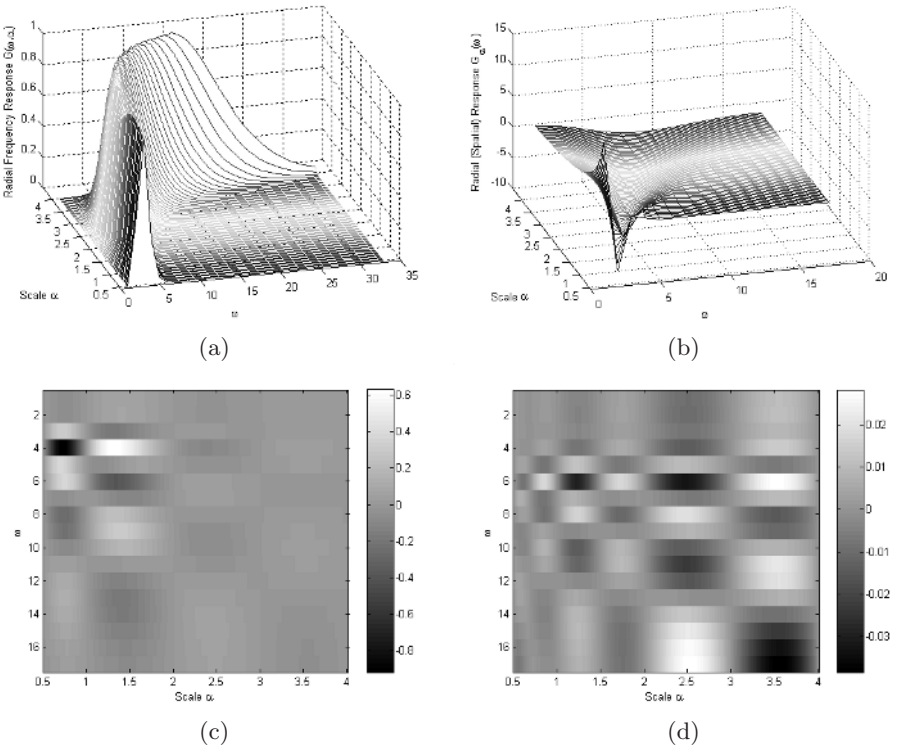

Fig. 1. From left to right: (a) Radial frequency response in the Fourier domain over scales α; (b) Real part of the radial response in the spatial domain over scales; (c) Error in the real part of the steered radial response from basis filters at scales 0.5, 1.0, 2.0, 3.0, 4.0; (d) Error in the real part of the steered radial response from basis filters at scales 0.5, 0.7, 1.0, 1.5, 2.0, 3.0, 4.0. Please note that the range of radial responses in (b) is $[-7.69, 13.31]$.

where $\mathbf{F}$ is a matrix of column vectors of the radial responses ($G_\alpha(\omega)$) in the spatial domain) across scales $[\alpha_1, \alpha_N]$ at very small intervals, $\mathbf{F_B}$ is a matrix of column vectors of radial responses from the basis set with scales $\{\alpha_1, \ldots, \alpha_N\}$ and $\mathbf{S}$ is a matrix of column vectors of steering coefficients to obtain each column of $\mathbf{F}$ from a linear combination of $\mathbf{F_B}$. Given that we can synthesise the matrix $\mathbf{F}$ by varying the scale parameter α in Eqn (4) in very small increments between $[\alpha_1, \alpha_N]$ and we can also synthesise $\mathbf{F_B}$, we obtain $\mathbf{S}$ by the Moore-Penrose generalised inverse

$$\mathbf{S} = \mathbf{F_B}^{\dagger}\mathbf{F} \tag{7}$$

where

$$\mathbf{B}^{\dagger} = (\mathbf{B}^T\mathbf{B})^{-1}\mathbf{B}^T \tag{8}$$

We can also evaluate the accuracy of the learnt steering solution for a given basis filter set by re-evaluating the steered radial responses

$$\hat{\mathbf{F}} = \mathbf{F_B S} \tag{9}$$

and thus empirically choose the scales α_i of the basis filter set to obtain an acceptable steering accuracy.

In order to select the scales of our basis filter set, we observe that the radial frequency response $G_\alpha(\omega)$ changes smoothly with the scale parameter α as shown in Fig. 1(a). The change in radial response in the frequency domain increases exponentially with α. In the spatial domain (Fig. 1(b)), this translates into an inverse exponential rate of change for the real part of the radial response, where most of the change occurs at small values of α. Therefore, we dedicate more basis filters to the finer scales than the coarser scales. In Fig. 1(c), we show the steering error $\hat{\mathbf{F}} - \mathbf{F}$ resulting from filter scales chosen at integer intervals (except the finest scale to avoid any aliasing), i.e. scales $\alpha_i \in \{0.5, 1.0, 2.0, 3.0, 4.0\}$. The steering errors occur mostly at the finer scales because of the scaling properties of the Erlang function. As we dedicate more basis filters to the finer scales, i.e. $\alpha_i \in \{0.5, 0.75, 1.0, 1.5, 2.0, 3.0, 4.0\}$, the steering errors are spread out more evenly and the magnitude of the errors is significantly reduced. We henceforth use the latter set of scales for our basis filters. The size of the filter kernels in the spatial domain range from 9×9 to 60×60. Fig. 1 suggests that the range of scales over which the filter responses can be steered can be efficiently increased by adding coarser-scale basis filters over larger intervals of α.

Each N-element column of $\mathbf{S}$ in Eqn (7) contains the steering coefficients for the N basis filters to obtain filter responses at the corresponding scale α. Therefore, each of the N rows of $\mathbf{S}$ contains the finely sampled steering coefficients across scales for the N basis filters. We fit 12^{th} order polynomial functions to regress the steering coefficients for each basis filter to the scale parameter α. We thus replace the steering coefficients $s_{i,\alpha}$ in Eqn (5) by polynomial steering functions[1] $s_i(\alpha)$ with polynomial coefficients cf_i^p where $p \in \{0, \ldots, 12\}$

$$s_i(\alpha) = \mathrm{cf}_i^{12}\alpha^{12} + \ldots + \mathrm{cf}_i^1\alpha + \mathrm{cf}_i^0 \tag{10}$$

to obtain

$$f_\alpha^\theta(x, y) = \sum_{i=1}^{N} s_i(\alpha) f_{\alpha_i}^\theta(x, y) \tag{11}$$

We show scale steering results on Jaehne's test image of radial cosine modulation with increasing frequency from the centre in Fig. 2. In order to show the accuracy of the complex steered responses, we show the energy (defined below in Eqn (16)) of the responses, which is independent of the phase of the cosine modulation, for orientation $\theta = 0$.

[1] We refer to the polynomial functions which provide the steering coefficients for a given basis filter from a scale parameter *alpha* as a *steering function*

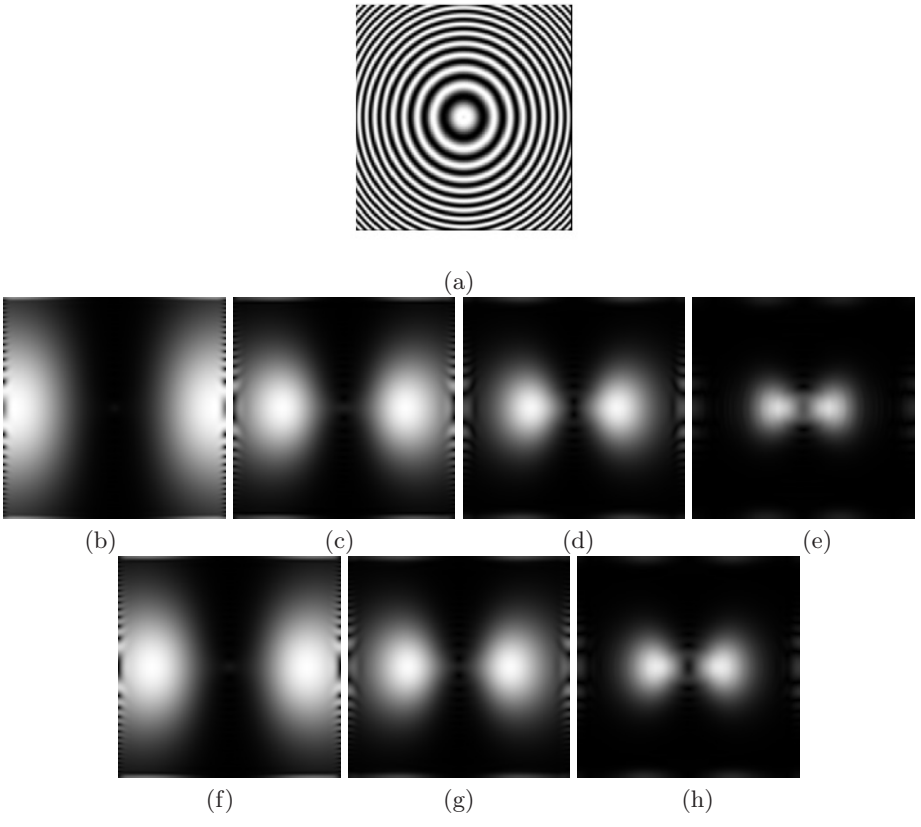

Fig. 2. From left to right: (a) Jaehne's test image with varying radial frequency; (b)-(e) Energy of the complex basis filter responses at scales $1.0, 1.5, 2$ and 3 for orientation $\theta = 0$ (vertical edges); and (f)-(h) Energy of the steered filter responses at intermediate scales $1.25, 1.75$ and 2.5 for orientation $\theta = 0$.

4 Detecting Intrinsic Scale

The polynomial steering functions allow one to obtain filter responses at any scale within the range of scales of the basis filter set. Kadir and Brady [4] have shown that normalised maxima of entropy over scales can be used to detect salient regions in images. Lindeberg [3] used normalised extrema in scale-space to detect edges and ridges more reliably. The formulation of the steering functions $s_i(\alpha)$ in terms of polynomial functions of α lends itself well to the detection of global maxima by analytically finding the roots of the derivatives of the polynomials, rather than exhaustively performing operations over multiple scales to detect maxima as in the previous aforementioned works.

Once the complex filter responses $f_\alpha^\theta(x, y)$ have been computed over an image, they can be treated as constants. A polynomial function multiplied by a constant

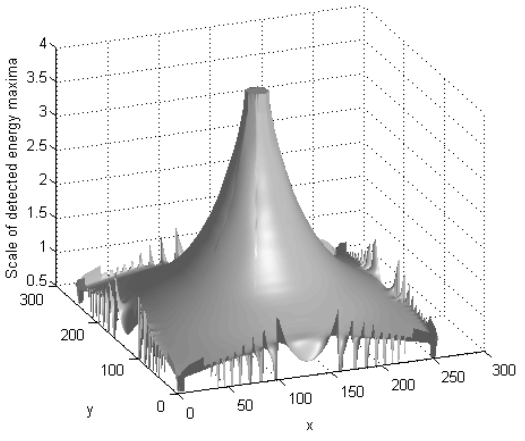

Fig. 3. Scale at which energy maxima were detected in Jaehne's test image, corresponding to the intrinsic scale function used to generate the test pattern. Note: Some noise at the borders remains even though filtering was done with border reflection.

results in a new polynomial function where the coefficients are scaled by the constant. We can thus multiply our polynomial steering functions $s_i(\alpha)$ by our field of filter response constants $f_\alpha^\theta(x,y)$ in Eqn (11) to obtain fields of polynomial steering functions for locations (x,y) in the image

$$f_\alpha^\theta(x,y) = \sum_{i=1}^{N} s_i^\theta(\alpha,x,y) \tag{12}$$

where

$$s_i^\theta(\alpha,x,y) = \left[\mathrm{cf}_i^{12} f_\alpha^\theta(x,y)\right]\alpha^{12} + \ldots + \left[\mathrm{cf}_i^{1} f_\alpha^\theta(x,y)\right]\alpha + \left[\mathrm{cf}_i^{0} f_\alpha^\theta(x,y)\right] \tag{13}$$

The filter responses over scales (Eqn (12)) can be further simplified by summing the polynomial functions $s_i^\theta(\alpha,x,y)$ (adding their coefficients) together for all basis filters i to obtain a field of single polynomial steering functions

$$f_\alpha^\theta(x,y) = s^\theta(\alpha,x,y) \tag{14}$$

where

$$s^\theta(\alpha,x,y) = \left[\sum_{i=1}^{N} \mathrm{cf}_i^{12} f_\alpha^\theta(x,y)\right]\alpha^{12} + \ldots + \left[\sum_{i=1}^{N} \mathrm{cf}_i^{1} f_\alpha^\theta(x,y)\right]\alpha + \left[\sum_{i=1}^{N} \mathrm{cf}_i^{0} f_\alpha^\theta(x,y)\right] \tag{15}$$

In essence, the weighted summation of a set of polynomial functions of the same variable α for steering across scales (Eqn (11)) can be simplified into a single polynomial function by weighting and summing the polynomial coefficients only

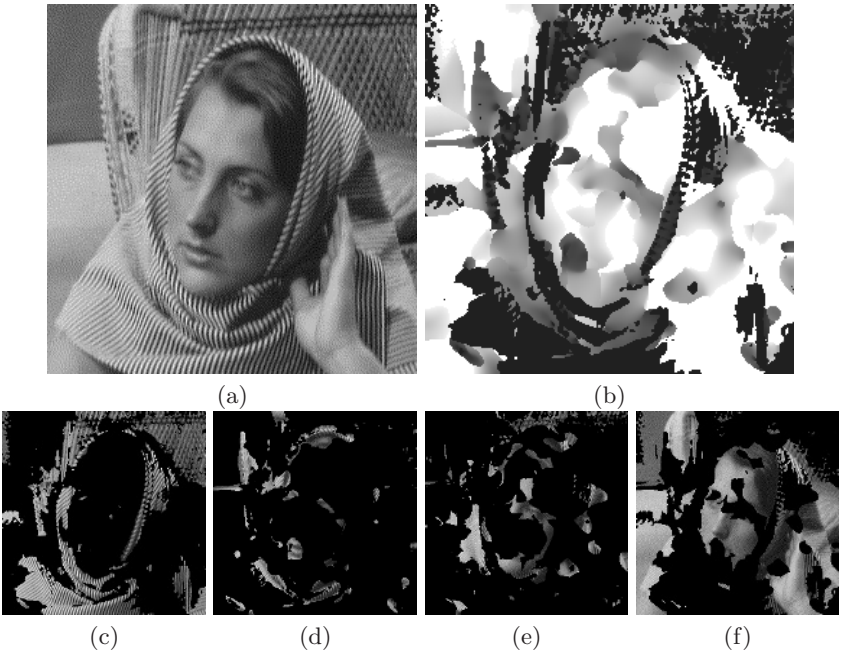

Fig. 4. From left to right, top to bottom:(a) Barbara image; (b) Map of energy maxima over scales (black is 0.5 and white is 4); Segmented Barbara image where energy maxima lies between scales (c) 0.5 and 1, (d) 1 and 2 , (e) 2 and 3, and (f) 3 and 4.

(commutation of operations). Finding derivatives of polynomial functions again only involves simple operations on the coefficients.

In order to search for phase-independent maxima of filter responses over scales, whereby ridge-like or edge-like image structures are treated equally, we need to obtain a steering equation for the energy of the complex response. The phase-independent "energy" response of a complex quadrature filter is obtained from the magnitude of the filter response $f_\alpha^\theta(x, y)$ [11]

$$E_\alpha^\theta(x, y) = \sqrt{real(f_\alpha^\theta(x, y))^2 + imag(f_\alpha^\theta(x, y))^2} \tag{16}$$

We can finally collapse the field of complex steering polynomial functions (Eqn (14)) by squaring[2] the real and imaginary parts of the polynomial steering functions in $f^\theta(\alpha, x, y)$ and adding them together. Obtaining the square root of a polynomial function is not a trivial task but fortunately, it is not needed because our final steering function $(E_\alpha^\theta(x, y))^2$ will have maxima at the same scales as $E_\alpha^\theta(x, y)$. To obtain an orientation-independent measure of energy maxima over scales, we select the maximum of the energy maxima in each of the four directions $\theta \in \{0, \frac{\pi}{4}, \frac{\pi}{2}, \frac{3\pi}{4}\}$. We show the results of the detection of energy maxima

[2] If the polynomial is represented as a vector of coefficients, convolving the vector with itself yields the square of the polynomial.

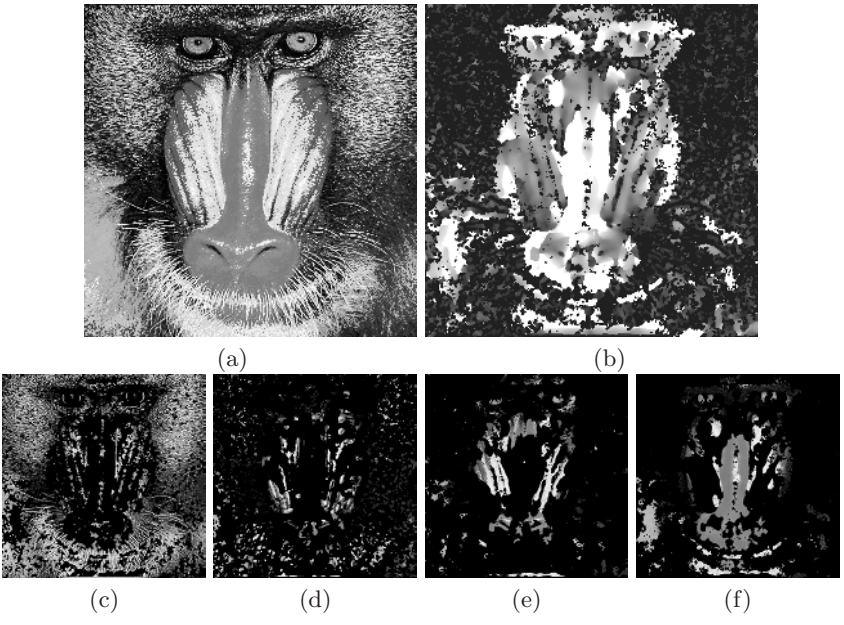

Fig. 5. From left to right, top to bottom:(a) Mandrill image; (b) Map of energy maxima over scales (black is 0.5 and white is 4); Segmented Mandrill image where energy maxima lies between scales (c) 0.5 and 1, (d) 1 and 2 , (e) 2 and 3, and (f) 3 and 4.

over scales (and a small set of fixed directions) in Jaehne's test image with varying radial frequency (scale of structures) in Fig. 3. We have used reflection along the borders of the image in order to obtain filtering results near the borders.

5 Experiments

We have applied our scale steering technique to detect maxima of phase-independent energy in popular images, such as Barbara and Mandrill, and other images of natural scenes where intrinsic scale plays an important part in identifying image structures. We show the scales at which energy maxima occur in different parts of the image and show preliminary results in coarsely segmenting the image into four bands: (a) $0.5 - 1.0$ for very fine scale structures such as texture, (b) $1.0 - 2.0$ for fine scale structures, (c) $2.0 - 3.0$ for medium scale structures, and (d) $3.0 - 4.0$ for coarse scale structures such as homogenous regions.

In the case of the Barbara image (Fig. 4), the stripes of Barbara's head-scarf and the hatched pattern of the chair in the back have been identified as very fine scale structures, shown in Fig. 4(c). Some folds of the head-scarf, the eyes and the mouth of Barbara have been segmented into the fine scale structures in Fig. 4(d). Barbara's chin and a blurred patch of the striped scarf have been segmented into medium scale structures. Finally, the forehead, the nose, the

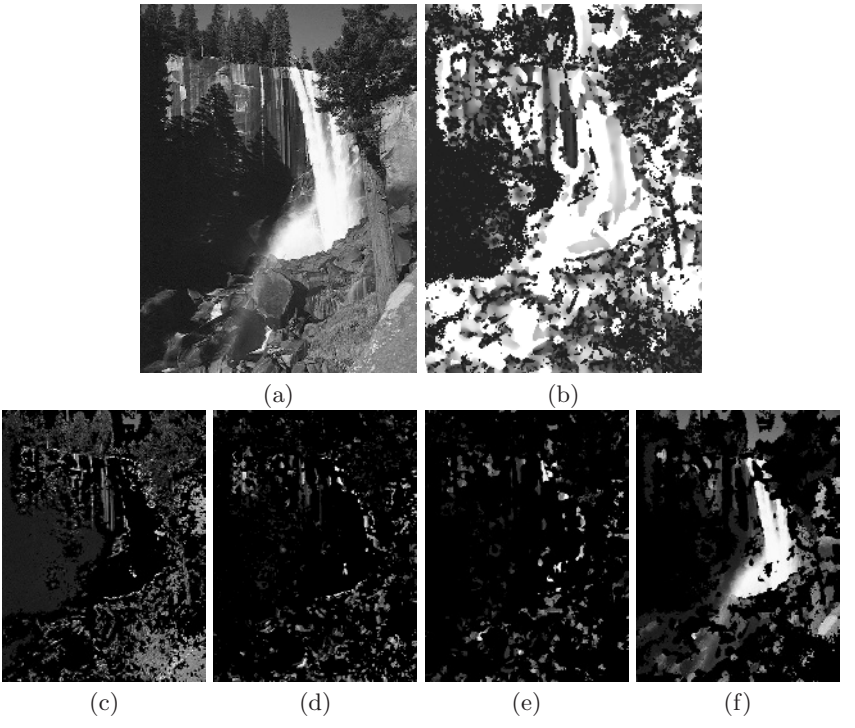

Fig. 6. From left to right, top to bottom:(a) Waterfall image; (b) Map of energy maxima over scales (black is 0.5 and white is 4); Segmented Waterfall image where energy maxima lies between scales (c) 0.5 and 1, (d) 1 and 2 , (e) 2 and 3, and (f) 3 and 4.

cheeks, the hands, uniform parts of the wall and floor, and a small piece of scarf and hatched chair were segmented into coarse scale structures in Fig. 4(f).

The ability to segment facial features based on their intrinsic scale can further be seen on the Mandrill image in Fig. 5. The fur, the whiskers and the fine edges are segmented into (c) very fine scale structures. Parts of the nose and some fur are segmented into (d) fine scale structures. Interestingly, the sides of the nose and the eyes are segmented into (e) medium scale structures and the nose is mainly segmented into (f) a coarse scale structure. In Fig. 6, we show how the main waterfall feature is segmented into a (f) coarse scale structure while the trees are segmented into (c) very fine and (d) fine scale structures. Image structures in the sea picture (Fig. 7) are also broken down into (f) coarse structures such as the big waves and the sky, (e) medium structures such as the horizon and some clouds, (c) and (d) for the smaller waves.

6 Conclusion and Future Work

Spatial filters give the highest response when their scale matches that of the image structure being filtered. Filtering over multiple scales such as in scale-space

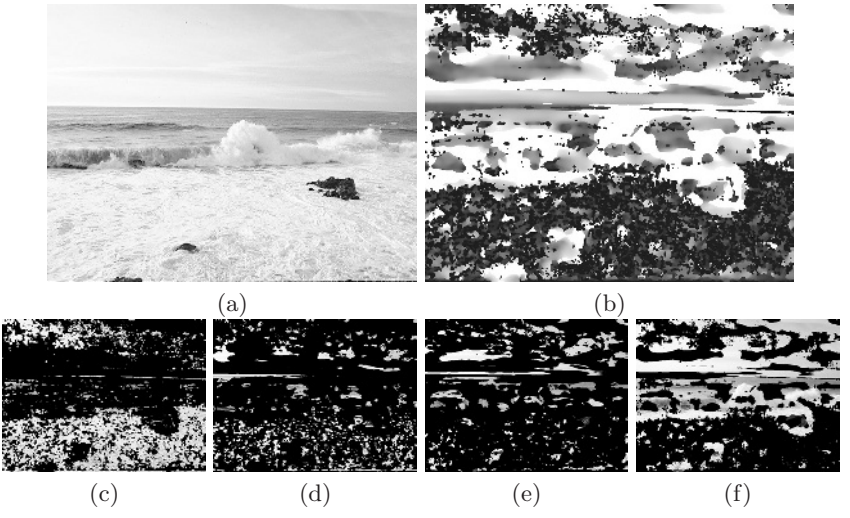

Fig. 7. From left to right, top to bottom:(a) Sea image; (b) Map of energy maxima over scales (black is 0.5 and white is 4); Segmented Sea image where energy maxima lies between scales (c) 0.5 and 1, (d) 1 and 2 , (e) 2 and 3, and (f) 3 and 4. Note that the segmentation has separated the clouds which are present in the sky.

representations and pyramids does not fully address the problem as the number of scales is usually constrained by computational power. We have described how to synthesise polar separable filters which possess quasi-invariant responses over scale by adopting Erlang functions as radial frequency characteristic. We have also shown how to create a basis filter set, learn the scale steering coefficients and evaluate the accuracy of the steering solution. The main novelty of our work lies in regressing the scale steering coefficients with polynomial functions and exploiting the ease of collapsing the linear combination of polynomial steering functions into a single polynomial function whose extrema can be analytically computed from the roots of its derivative. We have also shown that maxima of the energy response of our complex filters over scales correspond to the intrinsic scales of image structures both in Jaehne's test image and in natural images.

We have shown results where the global energy maxima over scales were found in each direction first and then the maximum energy over all filtered directions was chosen for determining intrinsic scale. We have not used the remaining roots of the polynomial functions which provide scale information about the other local energy maxima, minima and inflection points occurring both in the direction of greatest energy and the other directions. This information could potentially improve the segmentation results that we provided.

Acknowledgements. This work was funded by the UK Research Council under the Basic Technology Research Programme "Reverse Engineering Human Visual Processes" GR/R87642/02.

References

1. Simoncelli, E., Freeman, W.: The steerable pyramid: A flexible architecture for multi-scale derivative computation. In: IEEE Second International Conference on Image Processing. (1995)
2. Fdez-Valdivia, J., Garcia, J., Martinez-Baena, J., Fdez-Vidal, X.: The selection of natural scales in 2d images using adaptive Gabor filtering. IEEE Transactions on Pattern Analysis and Machine Intelligence **20** (1998) 458–469
3. Lindeberg, T.: Principles for automatic scale selection. In: Handbook on Computer Vision and Applications. Volume 2. Academic Press (1999) 239–274
4. Kadir, T., Brady, M.: Scale, saliency and image description. International Journal of Computer Vision **45** (2001) 83–105
5. Bredfelt, C., Ringach, D.: Dynamics of spatial frequency tuning in macaque v1. Journal of Neuroscience **22** (2002) 1976–1984
6. Lindeberg, T., Bretzner, L.: Real-time scale selection in hybrid multi-scale representations. In: Scale Space 2003. Volume 2695 of Lecture Notes in Computer Science. (2003)
7. Crowley, J., Riff, O.: Fast computation of scale normalised gaussian receptive fields. In: Scale Space 2003. Volume 2695 of Lecture Notes in Computer Science. (2003) 584–598
8. Freeman, W.T., Adelson, E.H.: The design and use of steerable filters. IEEE Transactions on Pattern Analysis and Machine Intelligence **13** (1991) 891–906
9. Perona, P.: Deformable kernels for early vision. IEEE Transactions on Pattern Analysis and Machine Intelligence **17** (1995) 488–499
10. Bharath, A.A.: Scale steerability of a class of digital filters. Electronics Letters **34** (1998) 1087–1088
11. Granlund, G., Knutsson, H.: Signal Processing for Computer Vision. Kluwer Academic Publishers (1994)
12. Witkin, A., Terzopoulos, D., Kass, M.: Signal matching through scale space. International Journal of Computer Vision **1** (1987) 133–144
13. Duits, R., Felsberg, M., Florack, L., Platel, B.: α scale spaces on a bounded domain. In: Scale-Space 2003. Volume 2695 of LNCS. (2003) 494–510
14. Papoulis, A.: Probability, Random Variables and Stochastic Processes. McGraw–Hill (1984)
15. Bharath, A.: Steerable filters from Erlang functions. In: British Machine Vision Conference. Volume 1. (1998) 144–153